



CHAPTER IV

DISCUSSION AND CONCLUSION

4.1 Numerical calculation of the solution

Because of the complexity of the solution, a computer program has been developed for calculating the current velocity as predicted by Eq.(3.15). The program as shown in the appendix is designed to provide the velocity magnitude and direction as well as the velocity components for any value of wind stress, wave parameter and water depth.

Fig.1 and Fig.2 are curves plotted from program output, showing the relationship between the surface velocity and the value $k\delta$, for different value of the kh in the case of zero shear stress at the surface. Fig.1 shows the magnitude of the surface velocity while Fig.2 shows the direction.

Fig 3,4,5,6 and 7 show the vertical distribution of the velocity component for different value of $k\delta$. The curves in each figure are for a ratio of water depth to wave length. These curves are also for zero shear stress at the surface.

Although the solution includes the effect of non-zero shear stress, only the case of zero shear will be discussed in this chapter because the aim of this paper is to provide a solution for comparison with the to be revised orbital flow theory by Jiraporn.

4.2 Comparison with Madsen solution

Madsen's solution for infinite depth as given by Eq.(1.4)

might be considered the limits of our solutions as given by Eq.(3.15), as the water depth goes to infinity. The first term on the right hand side of Eq.(3.15) represents the current induced by the wind stress. The rest represents the transport current induced by waves. The limit of the first term as the water depth goes to infinity is the classical Ekman's current. Shown in Fig.1 and Fig.2 are sets of curves for different values of kh . The thickened curves are the curves for infinite depth which are found to be the same as those given by Eq.(1.4). This confirms the correctness of the mathematical manipulator done in Chapter 3.

4.3 Effect of water depth on the speed and direction of wave-induced surface drift

As shown in Fig.1 and Fig.2 the surface drift speed depends very much on the water depth to wave length ratio. For relatively large depth, the drift speed is approximately proportional the ratio of Ekman's depth to wave length. For small value of depth to wave length ratio the speed is approximately proportional the Ekman's depth to wave length ratio up to a limit. After that the speed trend to become independent on Ekman's depth to wave length ratio.

With regard to the direction of the surface drift, the deflection angles as shown by curves in Fig.2 are in the range between 36 to 45 degree for deep water depth. For small water depth to wave length ratio, the deflection angle would be as low as a few degrees for large Ekman's depth to wave length ratio. For small Ekman's depth to wave length ratio the deflection angle oscillate around 45 angle.

011937



4.4 Conclusions

In this research paper the problem of current induced by wind stress and monochromatic waves in rotating ocean of finite depth has been theoretically investigated with the aim to provide a theoretical baseline for comparison with a new theory incorporating the concept of Coriolis moment by Jiraporn (1982). The governing equation used in the investigation is the same as that used by Madsen (1978). The current velocity gradient in the wind and wave direction at surface is assumed to be the sum of wind strain and the velocity gradient predicted by Longuet-Higgins' (1953) theory. The current velocity at bottom in the wind and wave direction is assumed to be the same as that predicted by Longuet-Higgins. The current velocity at bottom in the direction normal to the direction of wind and waves is assumed to be zero.

The solution to the governing equation is found to be in the same form as Madsen i.e. the current is composed of wind shear current and mass transport induced by waves. A computer program has been developed for calculating the speed and direction of the current predicted by theory. The curves plotted from the computer output shown that the theory is in conformity with Madsen's solution for the current of infinite depth.

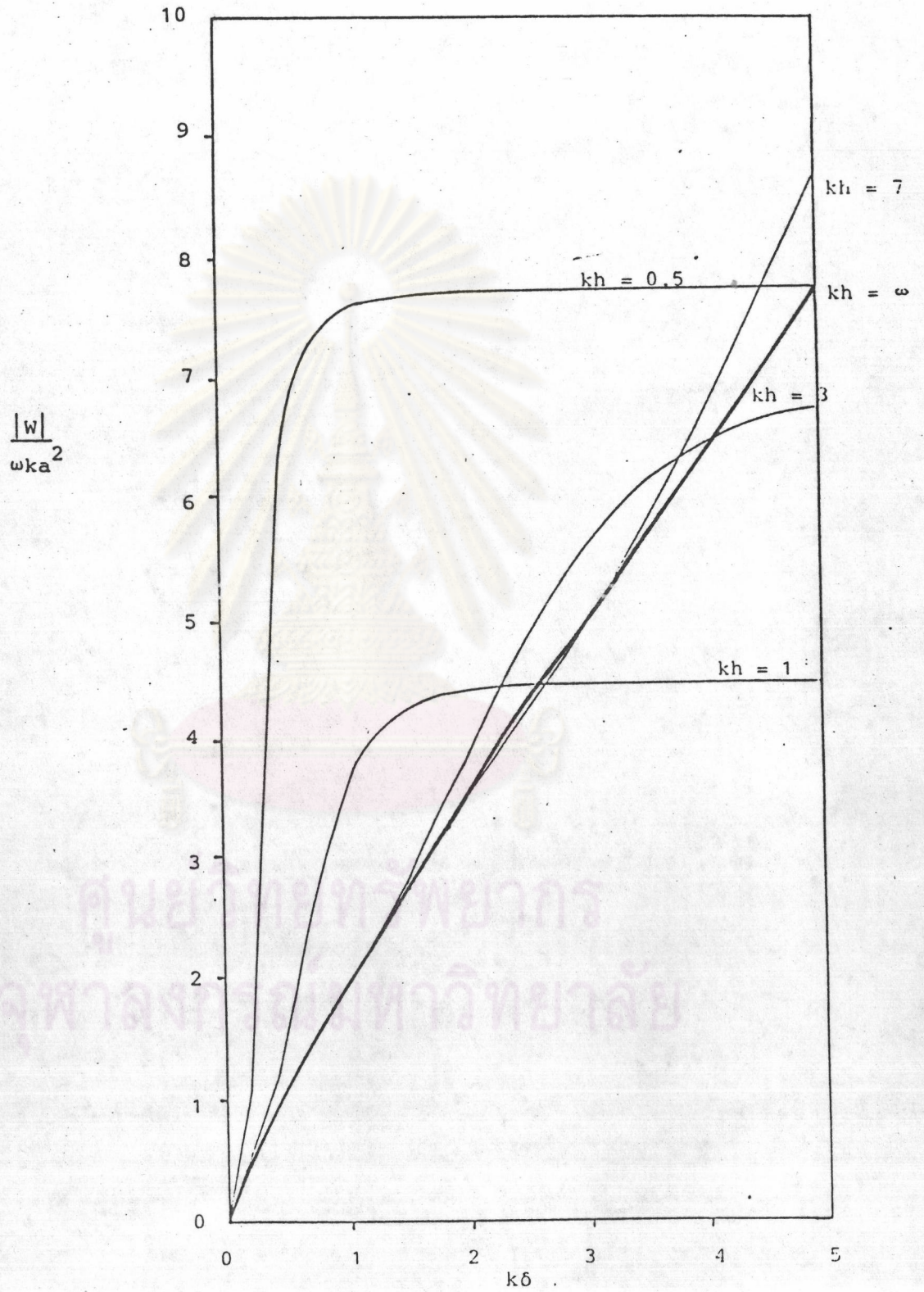


Fig. 1. Magnitude of the wave-induced surface drift as a function of $k\delta$

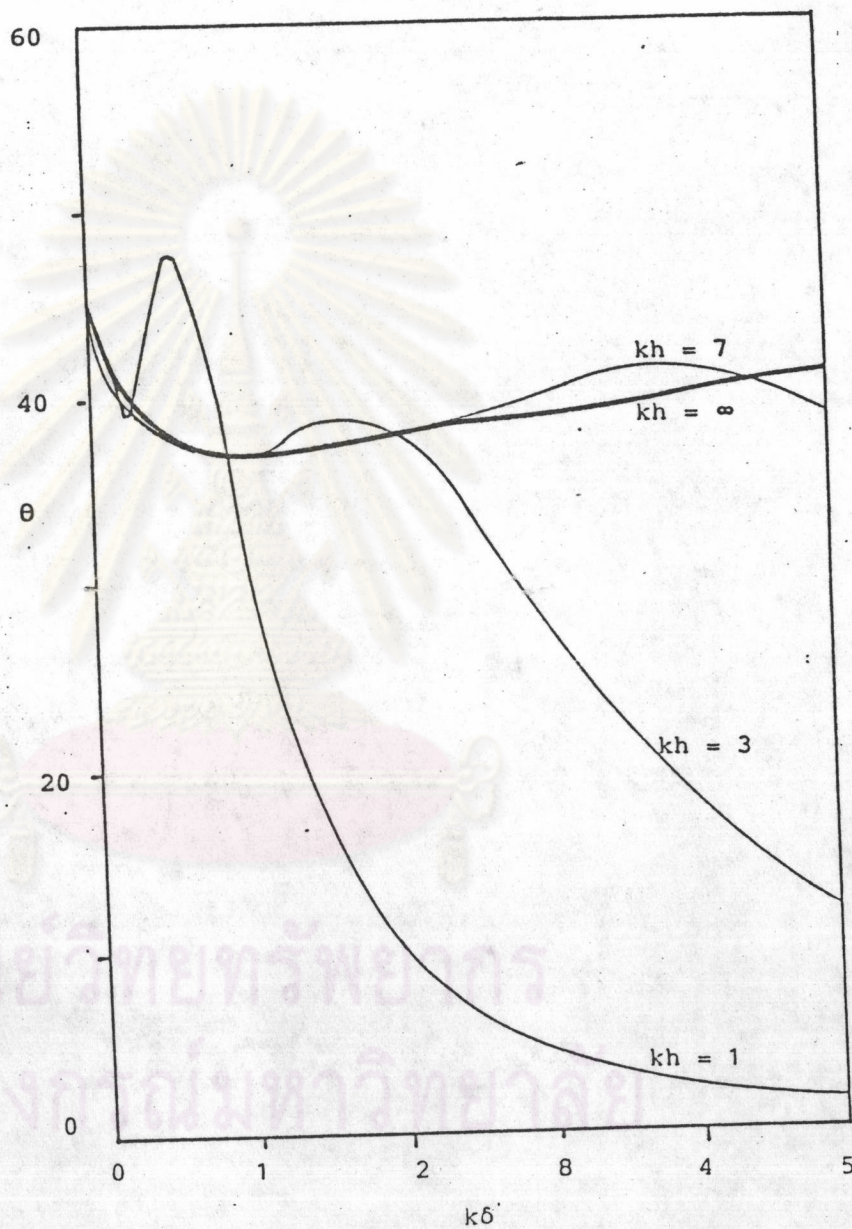


Fig. 2. Deflection angle of wave-induced surface drift relation to the wave and wind direction (deflection to the right on the Northern Hemisphere) as a function of $k\delta$

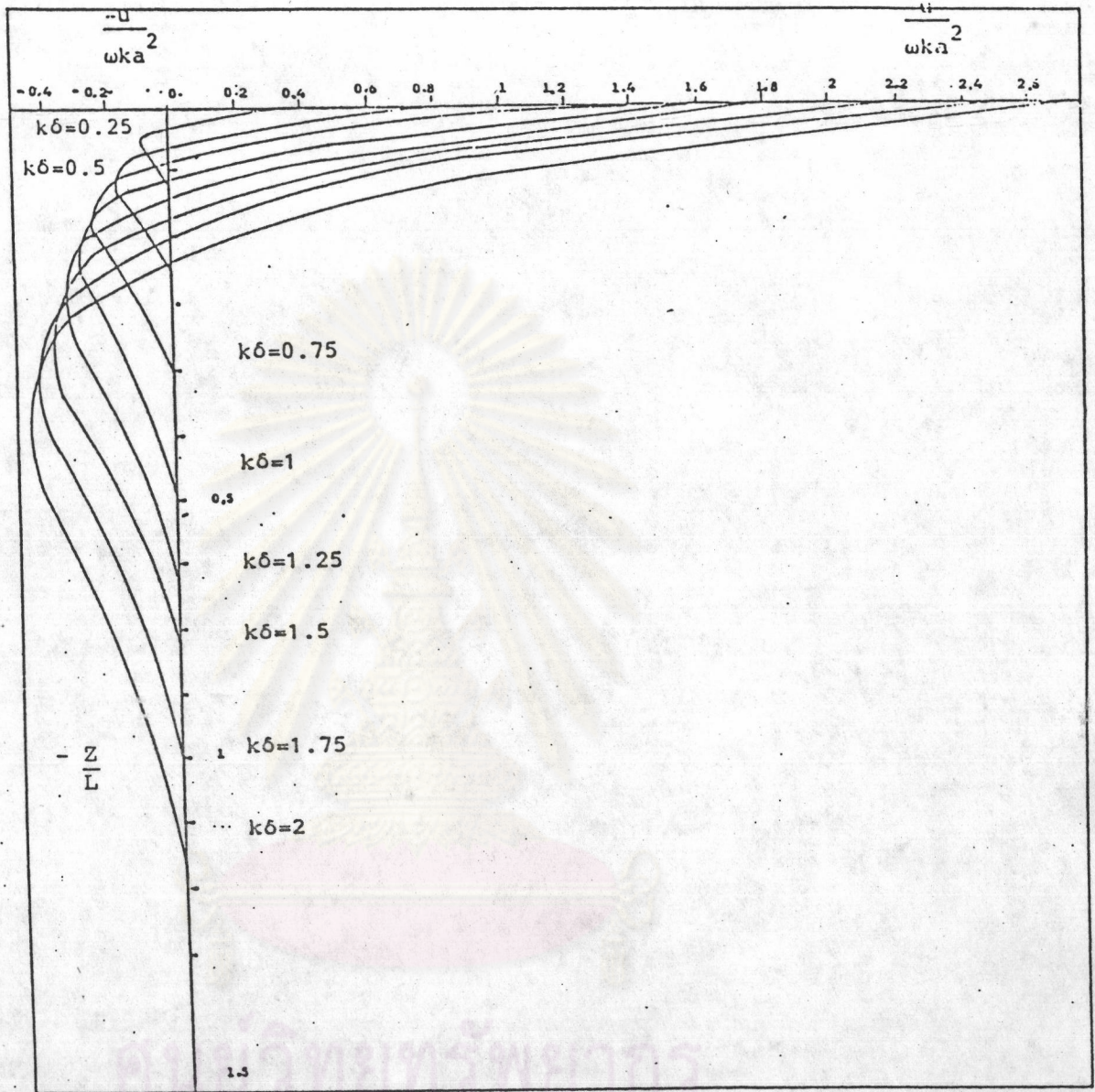


Fig. 3a Vertical distribution of the velocity component relation to $\frac{z}{L}$ in x-direction for $\frac{h}{L} = 1.5$

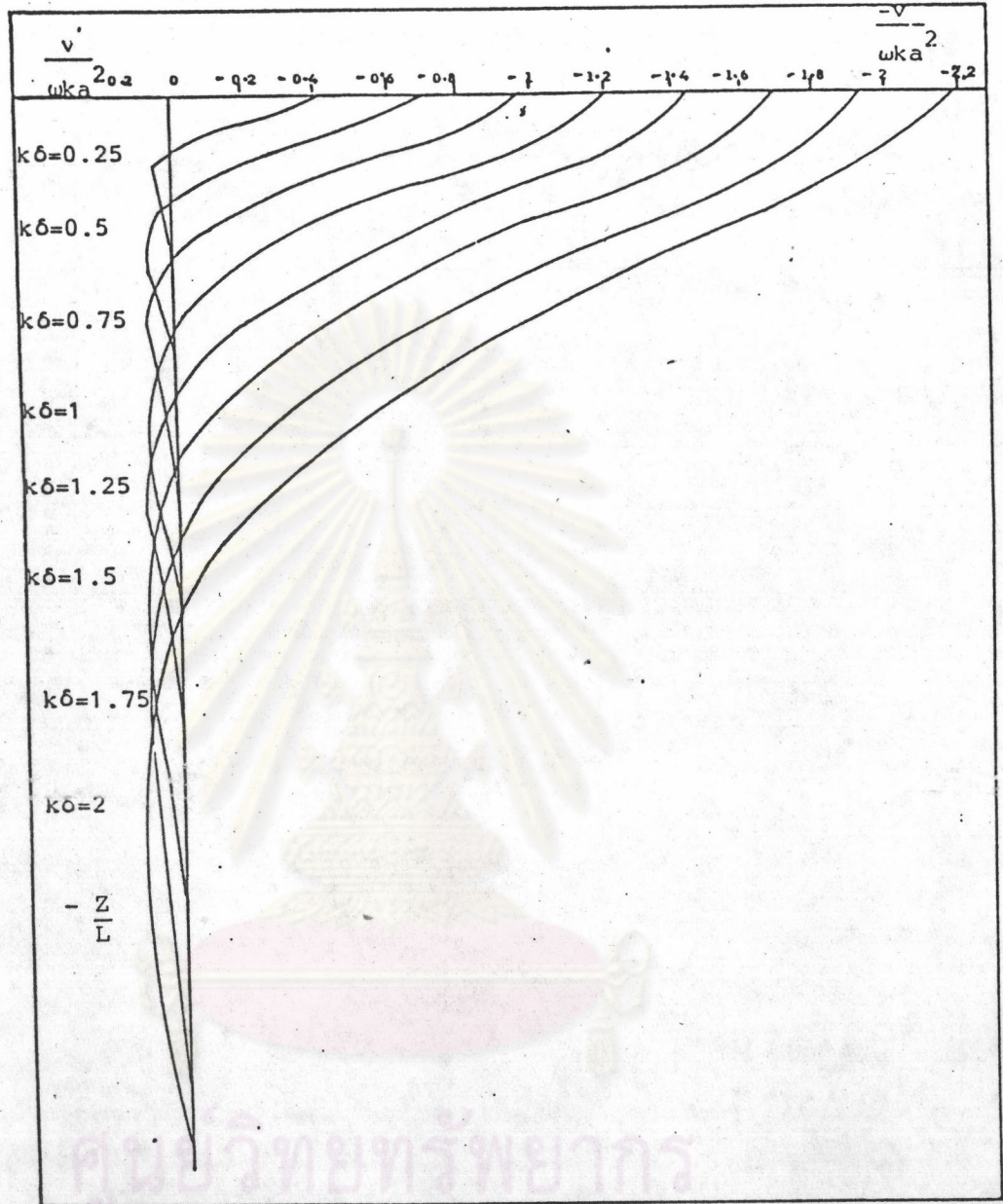


Fig . 3b Vertical distribution of the velocity component relation to $\frac{z}{L}$ in y-direction for $\frac{h}{L} = 1.5$

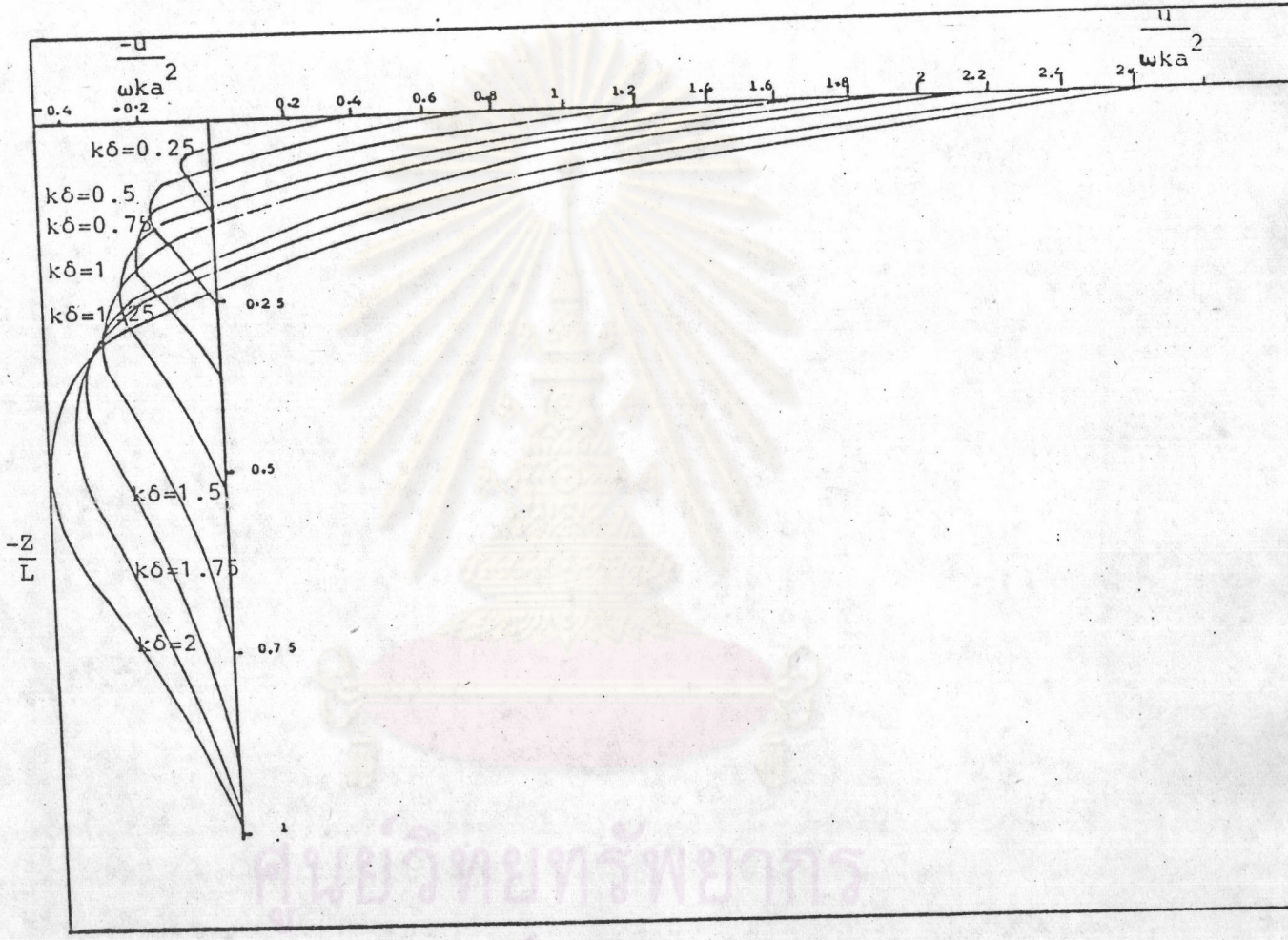


Fig. 4a Vertical distribution of the velocity component relation to $\frac{z}{L}$ in x-direction for $\frac{h}{L} = 1$

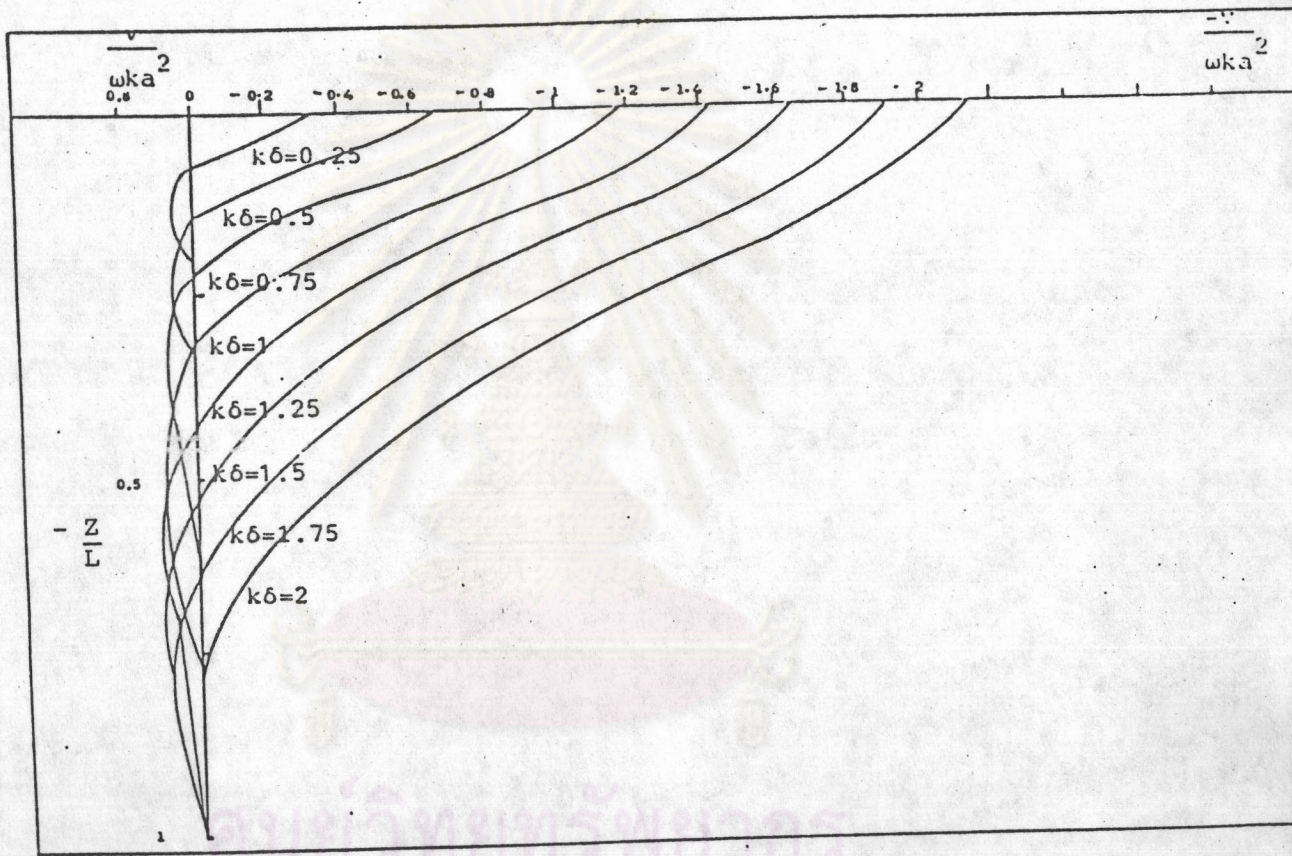


Fig. 4b Vertical distribution of the velocity component relation to $\frac{z}{L}$ y-direction for $\frac{h}{L} = 1$

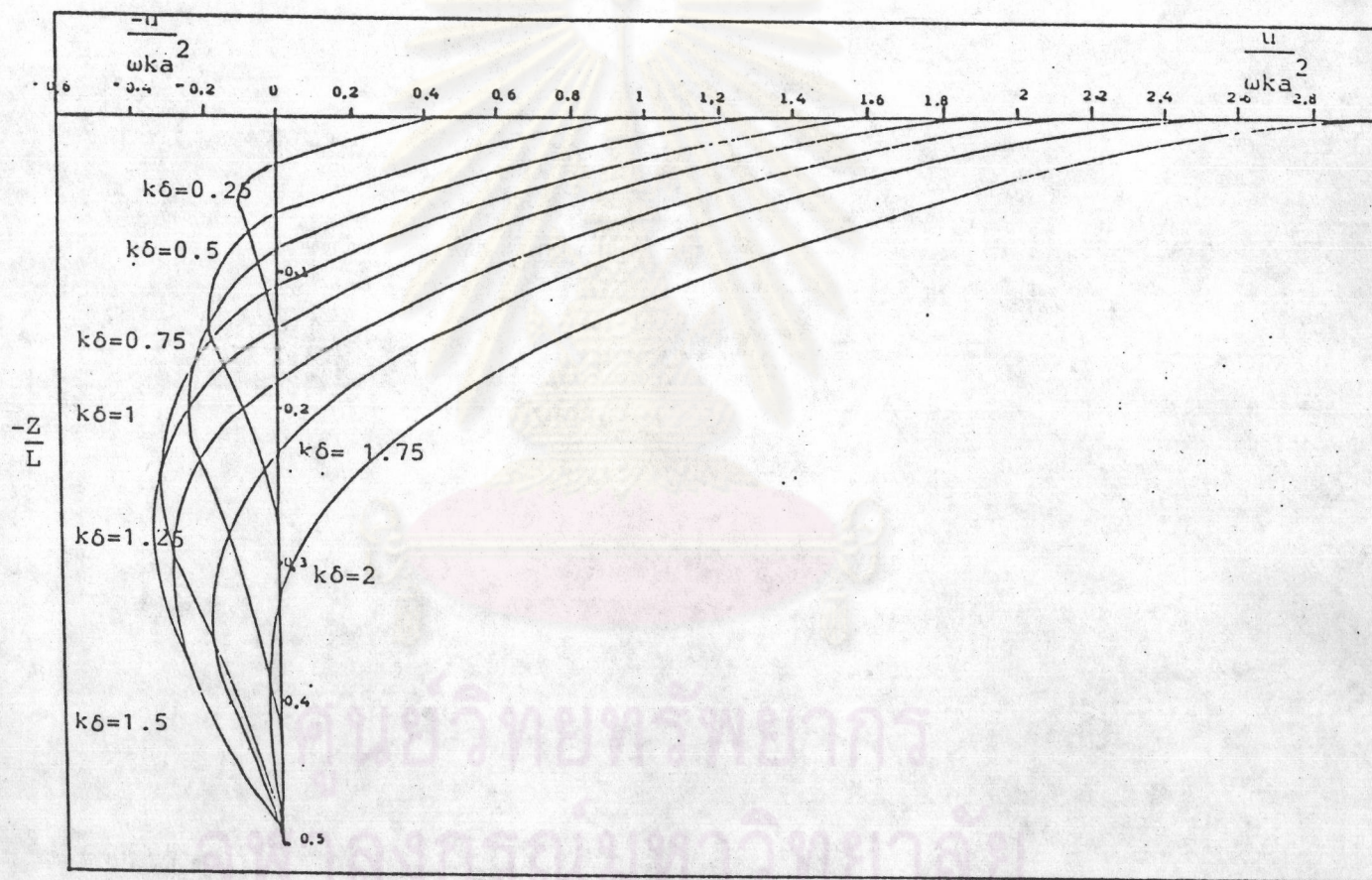


Fig. 5a Vertical distribution of the velocity component relation to $\frac{z}{L}$ in x-direction for $\frac{h}{L} = 0.5$

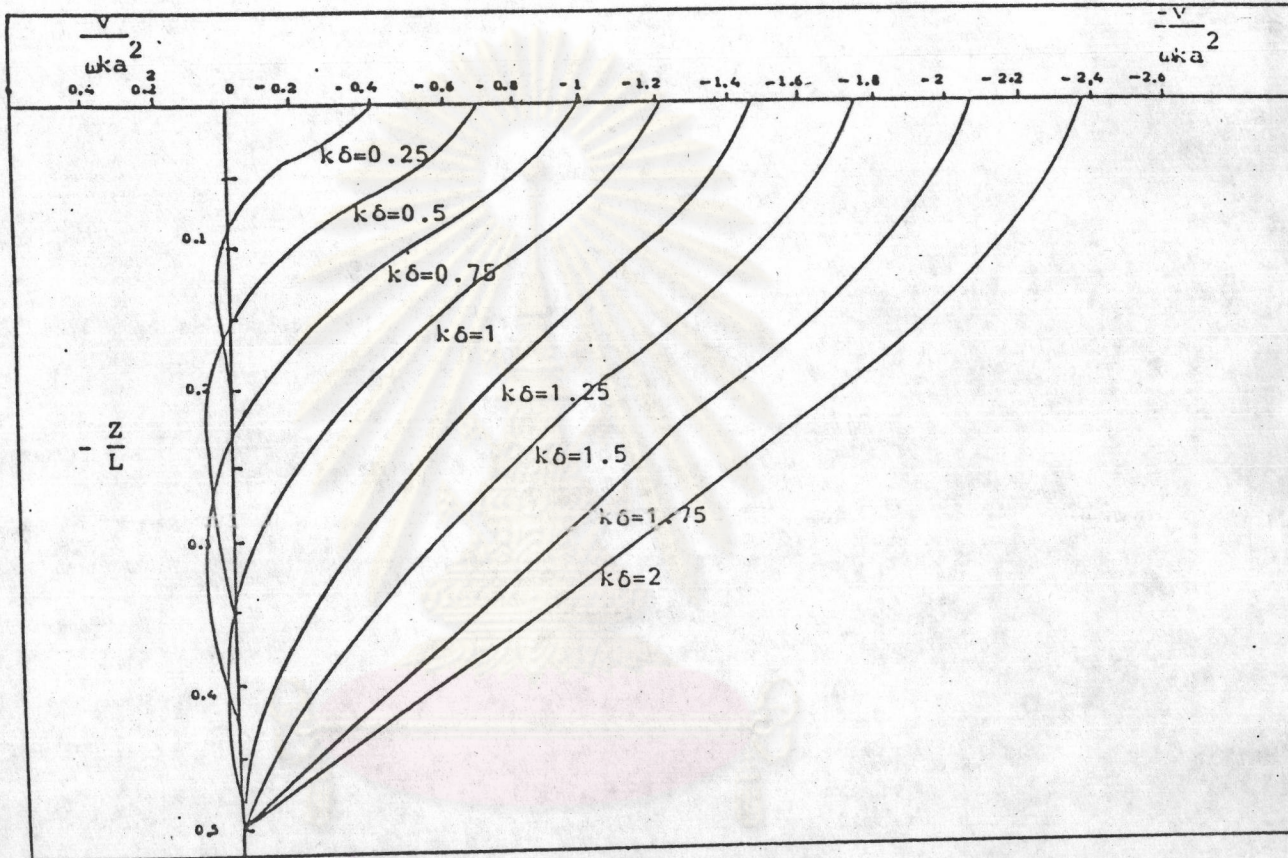


Fig. 5b Vertical distribution of the velocity component relation to $\frac{z}{L}$ in y-direction for $\frac{h}{L} = 0.5$

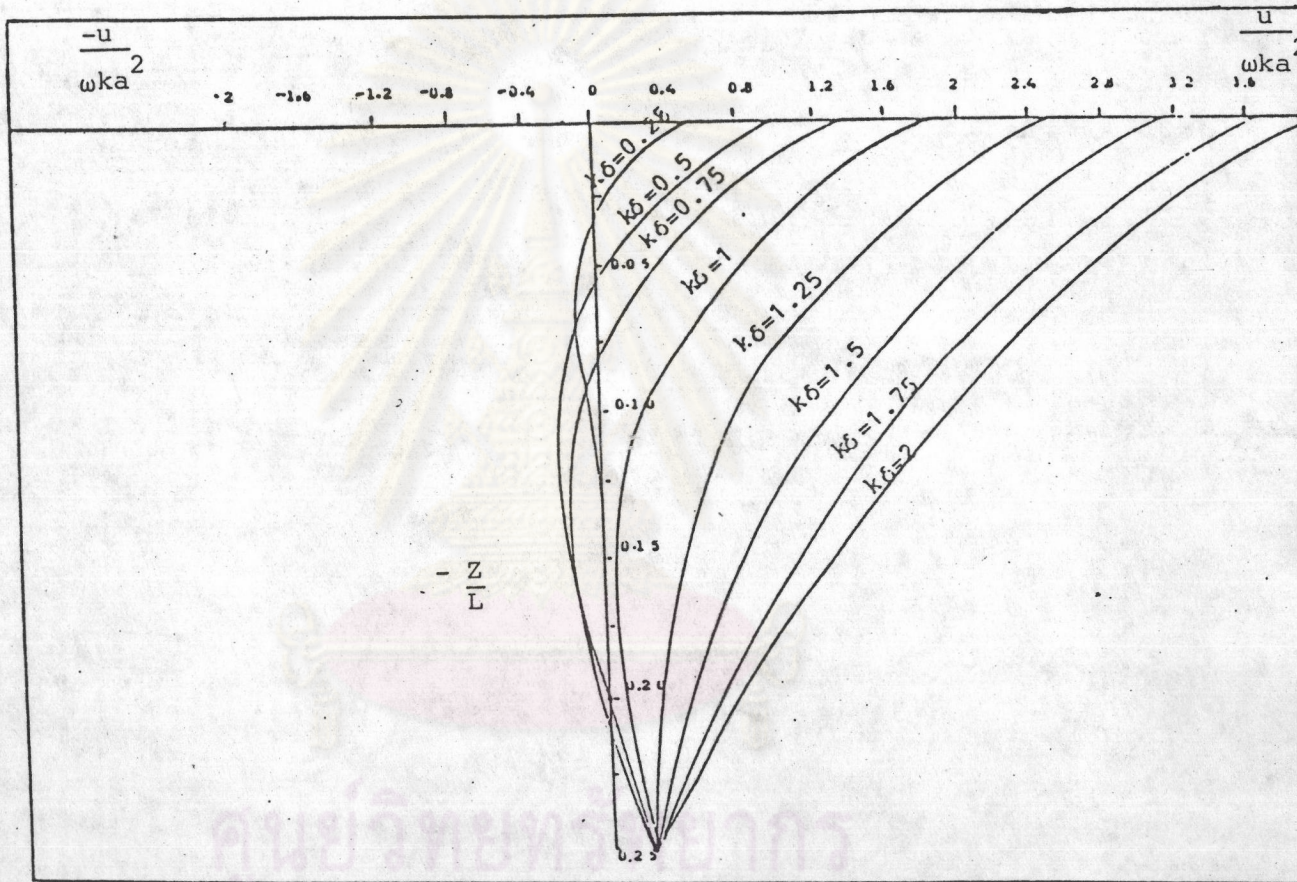


Fig. 6a

Vertical distribution of the the velocity componen
 relation to $\frac{Z}{L}$ in x-direction for $\frac{h}{L} = 0.25$

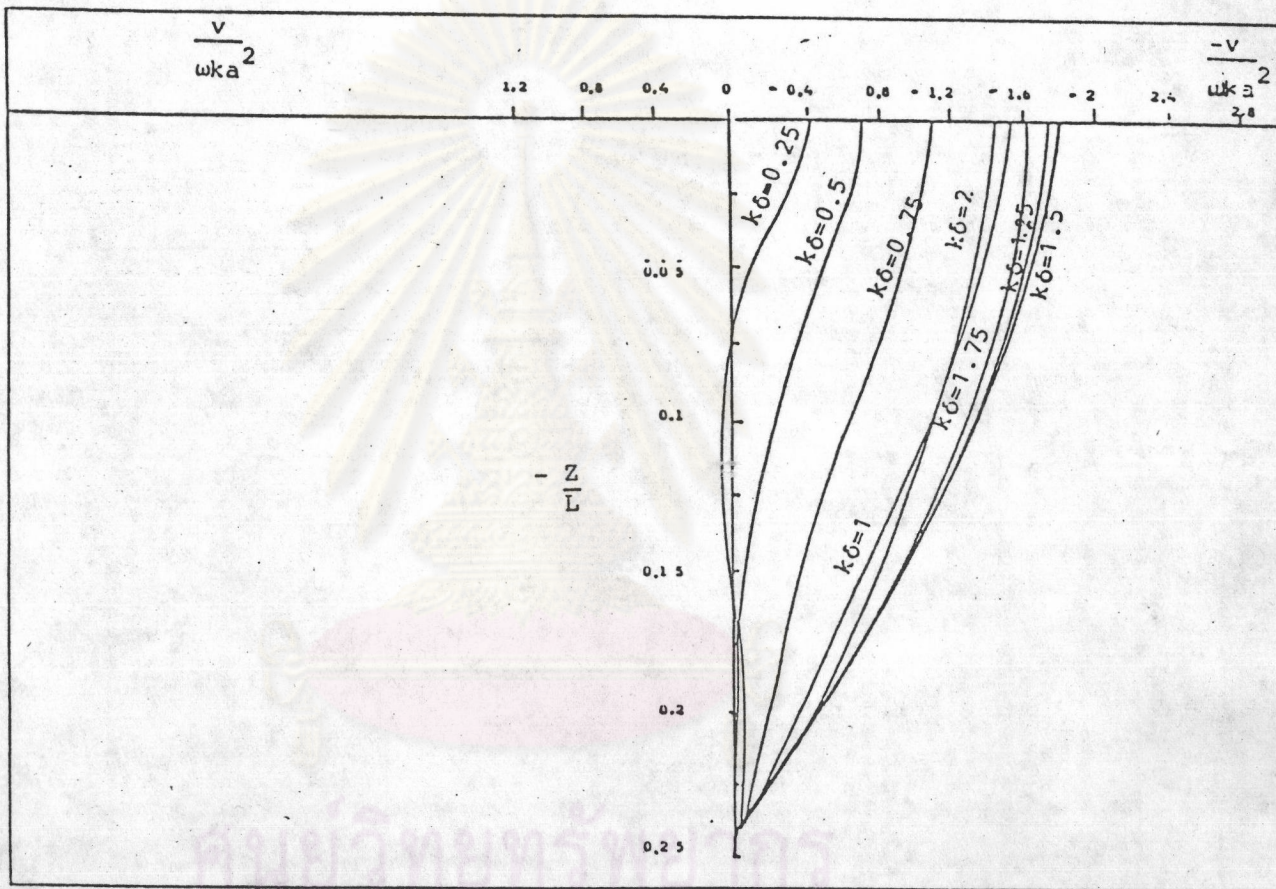


Fig. 6b Vertical distribution of the velocity component relation to $\frac{z}{L}$ in x-direction for $\frac{h_1}{L} = 0.25$

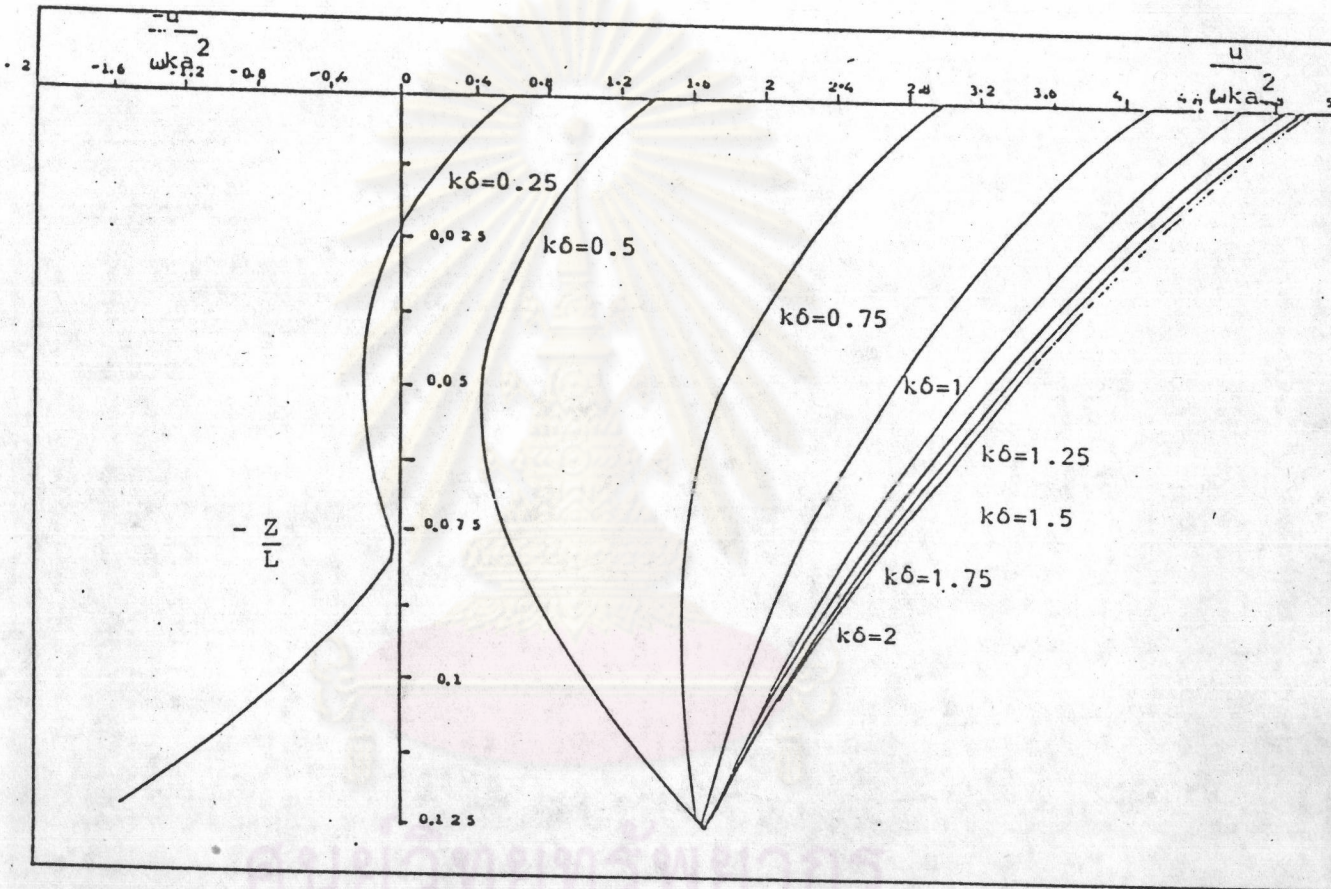


Fig. 7a Vertical distribution of the velocity component relation to $\frac{z}{L}$ in x -direction for $\frac{h}{L} = 0.125$

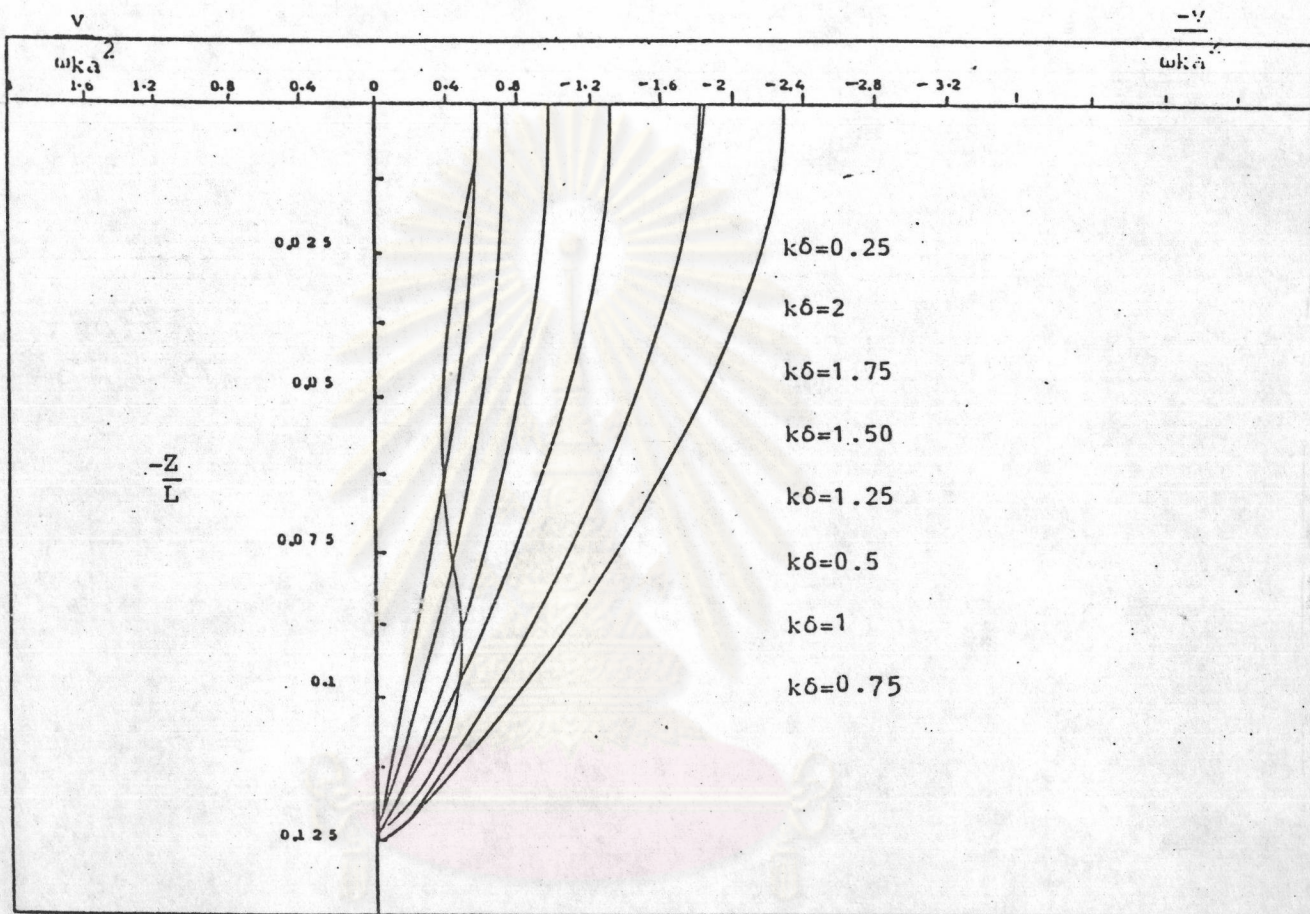


Fig. 7b Vertical distribution of the velocity component relation to $\frac{z}{L}$ in x-direction for $\frac{h}{L} = 0.125$